Available online at www.sciencedirect.com
SCIENCE DIRECT®

Journal of the European Ceramic Society 24 (2004) 533–540

www.elsevier.com/locate/jeurceramsoc

Microstructure and properties of porous β-SiC templated from soft woods

L. Esposito*, D. Sciti, A. Piancastelli, A. Bellosi

ISTEC CNR, Via Granarolo 64, 48018 Faenza (RA), Italy

Abstract

Porous β-SiC with a multimodal porosity preferentially oriented along one direction is obtained by infiltration of pyrolyzed wood with Si at $T > T_{\text{Si Melting}}$. Hard woods (obece, poplar and assembled poplar) are used as starting materials. The microstructure of the starting wood, of the wood after pyrolysis and after Si infiltration, is characterised in terms of overall porosity, pore size distribution and of crystallographic phases. The process is optimised for obtaining porous templates of only β-SiC with a microstructure that replicates the original wood microstructure. Features such as the presence of unreacted carbon, or conversely, of Si within the open pores of the infiltrated materials are minimized by a careful control of the amount of Si in contact with the carbon preform during the infiltration cycle. Compression tests on cubic samples are performed along the axial and longitudinal direction.

Keywords: Biomorphous materials; Compressive strength; Porosity; SiC; Wood precursors

1. Introduction

The process of *ceramization* of wood or of other biological structures is currently studied as an attractive way for the production of porous components with peculiar microstructures which cannot be obtained by means of other processes.[1] The intrinsic microstructure of the starting material is in fact replicated in a ceramic component. A wide range of ceramic materials can be produced and among these, porous SiC is particularly attractive for its high mechanical and thermal resistance.[2–4] In the typical process, dried wood is first carbonised to obtain a carbon perform, which is then siliconized in a way that gives porous SiC or Si/SiC composites.

Woods have a strongly anisotropic cellular structure with the majority of the pore channels oriented along one axis.[1] Porosity and morphology depend on the type of wood. All woods have a similar chemical composition: hemicellulose (10–20 wt.%), lignin (10–30 wt.%) and cellulose (30–55 wt.%). The structure of each channel is also quite similar and is formed by a series of layers each with a varying amount of the principal components. Because of these compositional and structural similarities, all woods behave similarly during the carbonisation process which therefore can be easily optimised. On the other hand each wood has a specific pore size distribution and such variety widens the applications of these materials: structures with an homogeneous pore size are required for filters, catalyst carriers or multifunctional membranes; heterogeneous structures can be used as biocatalyst support in the food industry or waste water treatment, for example.

Recent studies focussed on the optimisation of the two principal steps of the ceramization process for the production of porous SiC, pyrolysis of wood[5,6] and infiltration of the carbon perform with silicon (or silicon source).[7–12]

In the present study the behavior of two different woods in function of the temperature and time of infiltration with liquid silicon is presented. Obece (*Triplochiton scleroxylon*) and poplar (*Populus*) are selected because they are cheap and, in case of poplar, cultivated with no detrimental impact to the environment. Assembled poplar, obtained by carefully assembling selected sheets of poplar, is also tested because it is more homogeneous compared to poplar and therefore it can offer a higher resistance to the crack formation and propagation during the ceramization process.

* Corresponding author. Tel.: +39-0546-699748; fax: +39-0546-46381.
E-mail address: laura@istec.cnr.it (L. Esposito).

0955-2219/03/$ - see front matter © 2003 Elsevier Ltd. All rights reserved.
doi:10.1016/S0955-2219(03)00195-X

2. Experimental

Three commercial products were studied and compared: *Obece*, *Poplar* and *Assembled Poplar*, formed by sheets of wood assembled together.

Samples of about $60\times40\times30$ mm^3 were first dried at 70 °C for 24 h and then pyrolysed at 1000 °C for 1 h with heating and cooling rates of 1 °C/min and 2 °C/min, respectively, under flowing Ar in a graphite heating elements furnace. Infiltration cycles were conducted in the same furnace under flowing argon. The carbon templates (about 25×25 mm^2 and 10 mm high) were placed in a BN-coated graphite crucible and covered with silicon powder.

The first set of infiltration tests was conducted on pyrolysed *Obece* within the temperature range of 1450–1600 °C and soaking time range of 30–120 min in order to determine the best conditions for infiltration. The heating rate was 10 °C/min and the cooling rate was fast, obtained by switching off the furnace power. In order to study the degree of conversion, the amount of silicon powder also varied from 10 to 30% more than the stoichiometric quantity needed for the complete conversion from C template to SiC according to the reaction: $Si + C = SiC$. Finally, the influence of the wood structure orientation was also evaluated by changing the orientation of the template fibers from parallel to perpendicular with respect to the direction of the Si infiltration.

The infiltration tests on pyrolysed *poplar* and *assembled poplar* were conducted at 1500 °C×120 min, selected as the best processing conditions, with the wood channels parallel to the infiltration direction.

The porosity and pore size distribution of the as received, pyrolised and infiltrated specimens were measured by high-pressure mercury porosimetry using two different instruments: Pascal 140 Thermofinnigan for the porosity within the range 1.9–65 μm; Carlo Erba Porosimeter 2000 for the range 0.04–1.9 μm. The porosity of pyrolysed obece could not be evaluated with this instrument because, due to the poor mechanical resistance, the sample fractured during the mercury infiltration.

The relative amount of the crystalline phases in the infiltrated templates was calculated from the analysis of the X-ray diffraction patterns by comparing the relative intensities of the main peaks. The scattering factors used were 6.46[13] and 4.7,[14] for β-SiC and Si, respectively.

TG-DTA analyses were carried out (Netzsch GERAETEBAU STA409) on as received samples in order to determine the decompostion temperature of the woods.

Scanning electron microscopy equipped with energy dispersive spectroscopy (SEM-EDS) was used for the microstructural and elemental analysis of samples.

Image analysis (Image Pro Plus 4.0, Media Cybernetics, USA) on SEM micrographs was also used for the evaluation of pore size and distribution.

The degree of conversion was calculated according to the following relationship:

$$\text{Conversion degree}\,(\%) = W_{\text{final}} \cdot 100/[W_C \cdot Si_{AM}/C_{AM}]$$

where W_{final} is the weight of the template after the infiltration cycle, W_C is the weight of the carbon template, Si_{AM} and C_{AM} are the atomic mass of silicon and carbon, respectively. It must be taken into account, however, that the values obtained with this calculation neglect the presence of residual silicon into the porous template. The degree of conversion may result overestimated.

Compressive strength at room temperature was measured on samples $5.5\times6.5\times5.5$ mm^3 (height×width×length) using a crosshead speed of 1 mm/min. Samples were tested with the fibers oriented parallel and perpendicular to the compression direction.

3. Results and discussion

The pore size distribution and porosity of the as received samples, after pyrolysis and after infiltration at 1500 °C×120 min, are shown in Fig. 1 and Table 1.

3.1. The starting woods

The microstructure of the starting materials is revealed in Fig. 2. Poplar and obece have similar texture characteristics and pore dimensions. However, the longitudinal cross section of Obece (Fig. 2a) shows large and long channels ($\varnothing > 100$ μm) which are absent in poplar (Fig. 2b) and assembled poplar.

3.1.1. Obece

The porosity is 75.7% and the pore size distribution (Fig. 1a) reveals presence of micro-pores with a mean size of 0.5 μm and macro-pores of 18.3 μm. It must be noted however that these values do not take into account the big channels shown in Fig. 2a. In fact, pores with a mean size larger than 65 μm are not measured by the porosimeter previously described. The axial compressive strength is 30 MPa.[15]

3.1.2. Poplar

The porosity (71.6%) is similar to Obece and the pore size distribution is slightly bimodal (Fig. 1b). The size of micro and macro-pores of poplar resulting from the longitudinal section micrograph (Fig. 2b) is within the range of sensibility of the porosimeter and the mean size results 0.5 and 62.4 μm, respectively. Macro-pores are more numerous but smaller in poplar than in obece, whereas micro-pores have the same mean size but a wider distribution. Axial compressive strength is 31 MPa.[15]

3.1.3. Assembled poplar

The porosity (50%) is lower compared to the other woods and most of the pores are around 1 μm (Fig. 1c). The assembling process leaded to a more regular texture and a reduced porosity compared to the other woods.

3.2. The pyrolysis process

Table 2 reveals the weight loss and shrinkage values of the samples after pyrolysis. A massive weight loss (about 70%) and shrinkage (about 20–30%, depending on the direction) occurred in all samples, but none of them fractured or was reduced to powder. The curve obtained with the TG analysis under flowing argon is similar for all the woods and showed that the largest part of the overall weight loss occurred between 200 and 350 °C. The X-ray diffraction patterns reveal only amorphous carbon in all the pyrolysed specimens.

The porosity (Table 1) increases after pyrolysis as a consequence of the massive weight loss. The weight loss is only in part counterbalanced by the simultaneous shrinkage, as confirmed by the increase of the micro and macro-pore size. In the case of assembled wood, the increase of the porosity is particularly high (from 50 to 83%) because of the volatilisation of the organic compounds used during the assembling process.

The pore size distribution of poplar and assembled poplar after pyrolysis (Fig. 1b) is bimodal with a consistent amount of pores around 1 μm, which were absent before the pyrolysis. Such pores probably formed in consequence of the volatilisation of the compounds which in the wood obstructed the channels with a dimension around 1 μm.

The microstructure of the carbon templates replicates the microstructure of the original woods (Figs. 3a–b, 4a–b and 5a). Pyrolysed Obece (Fig. 3a–b) exhibits

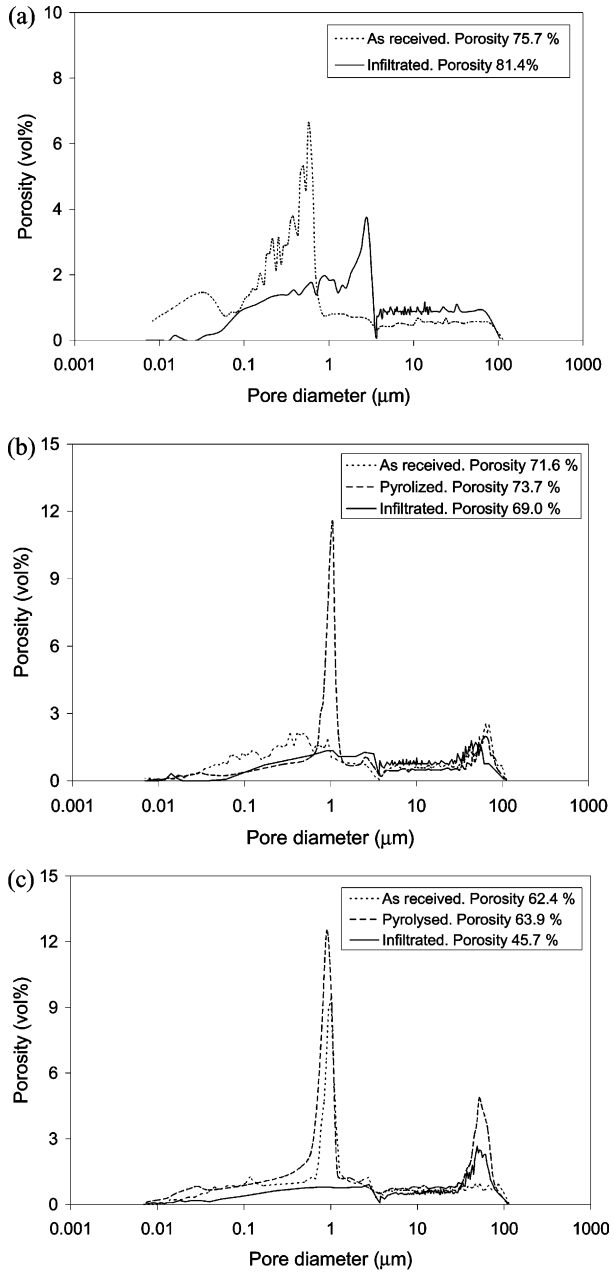

Fig. 1. Pore size distribution of as received samples, after pyrolysis at 1000 °C and after infiltration with silicon at 1500 °C×2 h: obece (a); poplar (b); assembled poplar (c).

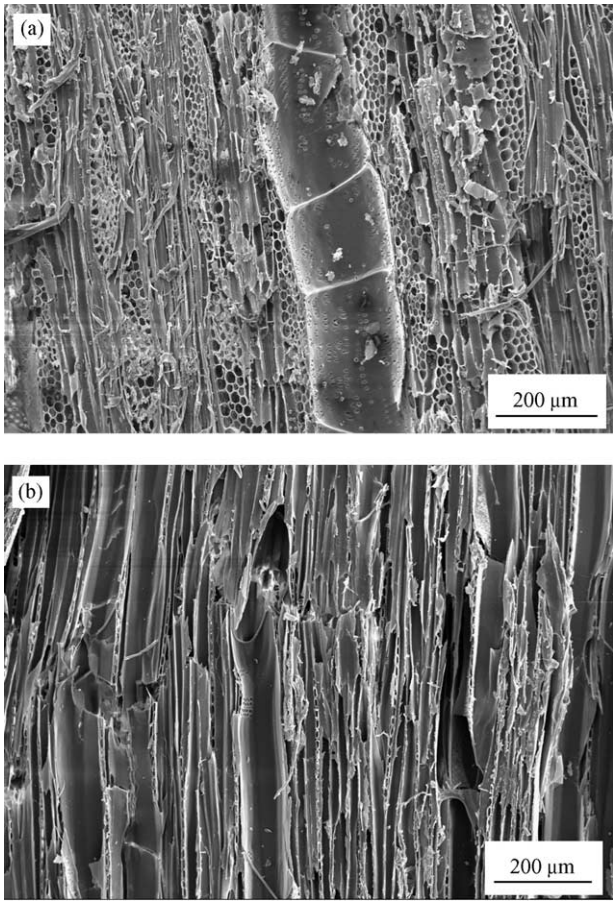

Fig. 2. Longitudinal section microstructure of obece (a) and poplar (b).

Table 1
Porosity of as received, pyrolised (1000 °C×1 h) and infiltrated (1500 °C×2 h) samples[a]

Sample	Obece			Poplar			Assembled poplar		
	Porosity (%)	Microp. M. size (μm)	Macrop. M. size (μm)	Porosity (%)	Microp. M. size (%)	Macrop. M. size (%)	Porosity (%)	Microp. M. size (%)	Macrop. M. size (%)
As received	75.7	0.5	18.3	71.6	0.5	62.4	50.0	1.0	31.9
Pyrolised	[b]	8.8[c]	80.4[c]	73.7	1.1	63.9	82.6	1.0	53.5
Infiltrated	81.4	3.0	18. 6	69.0	1.0	45.7	63.0	1.0	47.8

[a] Porosity range is 0.04–65 μm. Micro-pore range: 0.04–1.90 μm; macro-pore range: 1.9–65.0 μm.
[b] Sample fractures during mercury infiltration.
[c] Measure taken by Image Analysis on SEM micrograph.

macro and micro-pores of about 80 and 9 μm, respectively, as assessed by the image analysis technique. The micro-pore mean size is probably slightly overestimated with this technique since small pores are hardly identified in the micrographs. In addition, obece exhibits numerous small pores even along the radial direction (Fig. 2a), which are neglected in the calculation. The microstructure of pyrolysed Poplar (Fig. 4a and b) confirmed the bimodal pore size distribution revealed by the analysis with the porosimeter (Fig. 1b). The microstructure of assembled poplar after pyrolysis revealed the presence of numerous cracks along the interface between the wood layers (Fig. 5a) probably formed during the volatilization of the organic compounds used to assemble the layers together. The micro- and macro-pores have similar size and morphology as those of pyrolysed poplar.

3.3. The silicon infiltration process

Table 3 reassumes the results obtained with different infiltration cycles.

During the infiltration process with silicon the weight of the samples increased as a consequence of the Si entering by capillarity into the carbon template, leading also to a decrease of the porosity and of the pore mean size (Table 1).

According to Greil et al.,[1] the time required for the liquid silicon to penetrate by capillarity into carbon templates derived from woods, is in the range of seconds, whereas the reaction Si(l) + C(s) = SiC(s) occurs in a longer time. The reaction is therefore the rate limiting step of the process.

Table 2
Weight loss and shrinkage values after pyrolysis at 1000 °C×1 h

Sample	Weight loss (%)	Axial shrinkage (%)	Radial shrinkage (%)
Obece	70.6	22.2	24.2±1.0
Poplar	73.6	18.8	31.0±1.0
Assembled poplar	68.2	23.4	30.0±2.0

The maximum diameter of the capillary for the infiltration with liquid silicon is about 80–120 μm,[1] which is within the pore size range of the woods selected in the present study. Experiments reported in literature revealed that when carbon templates derived from various types of wood were infiltrated with liquid silicon, pore channels up to 30 μm were generally filled with silicon after the infiltration cycle.[3,7] In the infiltration tests described in the following, in order to avoid the formation of Si–SiC composites rather than porous, pure β-SiC, the total amount of silicon powder was carefully controlled and limited to 10–30 wt.% more than the stoichiometric quantity needed for the complete conversion of the carbon preform.

3.4. Infiltration tests with pyrolysed obece

A summary of the relevant tests is reported in Table 3. The microstructure of obece after infiltration at 1500 °C×2 h is revealed in Fig. 3c and d.

Infiltration at 1600 °C for 30 min (sample 1) results in a low degree of conversion (75.9%) of Si and C to SiC. A possible explanation is that at 1600 °C the volatilisation of Si is favoured under low PO_2 condition[16] and therefore part of the silicon is transformed into gaseous Si or SiO before reacting with the carbon template. The X-ray diffraction pattern shows only β-SiC peaks but, considering the low degree of conversion, amorphous carbon is probably present in this sample.

Infiltration at 1450 and 1500 °C (samples 2–6) overcomes the problem of the Si volatilisation but a longer holding time (120 min) is required to complete the Si + C = SiC reaction. Specimens treated at these temperatures exhibited a much higher degree of conversion (from 94 to 100%).

Samples 2, 3 and 4 were treated at 1500 °C×2 h. The amount of β-SiC increases from 85.5 to 100 vol.% by increasing the silicon in excess from 18.1 to 27.7 wt.%. The microstructure of sample 3 (Fig. 3c and d) is characterised by few macro-pores and homogeneous micro-pores which give a quasi-monomodal pore size distribution (Fig. 1a). The amount of residual silicon is rather low, 10.4 vol.%, as confirmed by microstructural

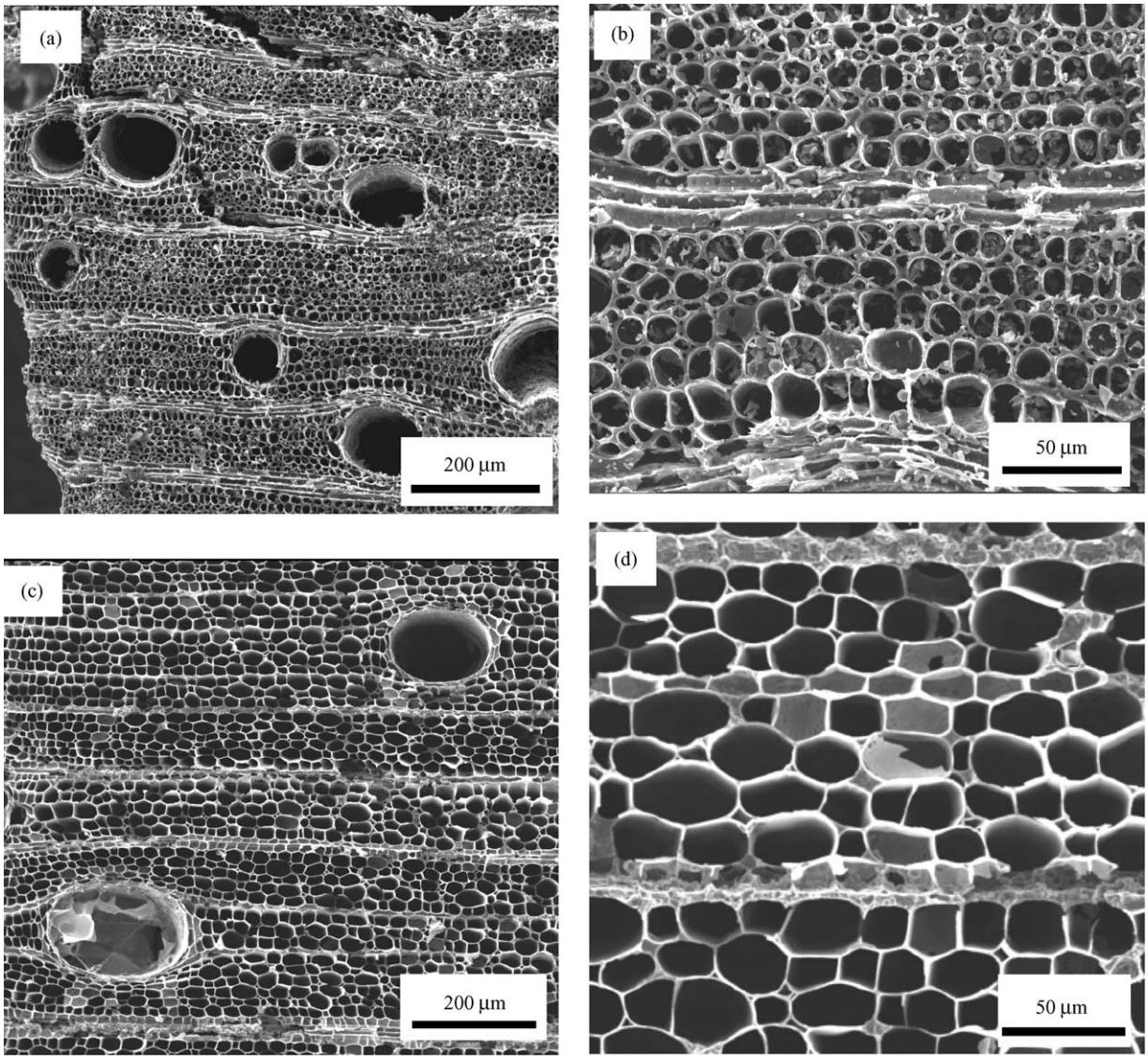

Fig. 3. Cross section microstructure of obece after pyrolysis at 1000 °C×1 h (a,b) and after infiltration with Si at 1500 °C×2 h, sample 3 of Table 3 (c,d).

Table 3
Results obtained with different infiltration cycles of the carbon templates with liquid silicon

Sample	Starting wood	Infiltration cycle (°C×min)	Excess of Si (wt.%)	Degree of conversion (%)	Crystalline phases	
					β-SiC (vol.%)	Si (vol.%)
1	Obece	1600×30	12.8	75.9	100	
2	Obece	1500×120	18.1	93.6	85.5	14.5
3	Obece	1500×120	20.5	101.5	89.6	10.4
4	Obece	1500×120	27.7	93.6	100	0.0
5	Obece	1450×120	13.2	96.5	71.6	28.4
6[a]	Obece	1450×120	16.0	97.8	64.5	35.5
7	Poplar	1500×120	28.3	97.3	71.9	28.1
8	Ass. poplar	1500×120	21.7	79.3	73.5	26.5

[a] Sample with fibers oriented perpendicularly to direction of the Si penetration.

analysis (the great majority of pores are open) and by the elevated porosity (81.4%).

Sample 5 and 6 were treated at 1450 °C×2 h. The relatively high level of residual silicon (28.4 and 35.5 vol.% respectively) is due to the temperature-dependence of the Si + C = SiC reaction. After 2 h at 1450 °C the reaction is not completed. In addition, the orientation of wood channels in respect of the direction of infiltration did affect the ceramization process: sample 6, which was infiltrated with the channels oriented in the opposite direction with respect to the silicon penetration front, exhibited a higher amount of residual silicon. The resulting microstructure is not homogeneous, with some regions that did not react, others that showed a remarkable cell wall thickening and the closure of the smaller pores with silicon.

3.5. Infiltration tests with pyrolysed poplar and assembled poplar

Pyrolysed poplar and assembled poplar were infiltrated at 1500 °C×2 h, as these were the conditions which gave the best results in case of obece. The microstructure of samples is revealed in Figs. 4c and d and 5b.

The porosity and macro-pore mean size of both samples decreased compared to pyrolysed samples as a consequence of the silicon infiltration and reaction with carbon (Table 1). Further, the amount of micro-pores decreased, as shown by the pore size distribution curves in Fig. 1b and c. A similar behavior is expected for obece, although a direct comparison is not possible since, as mentioned before, the porosity of pyrolysed obece could not be measured.

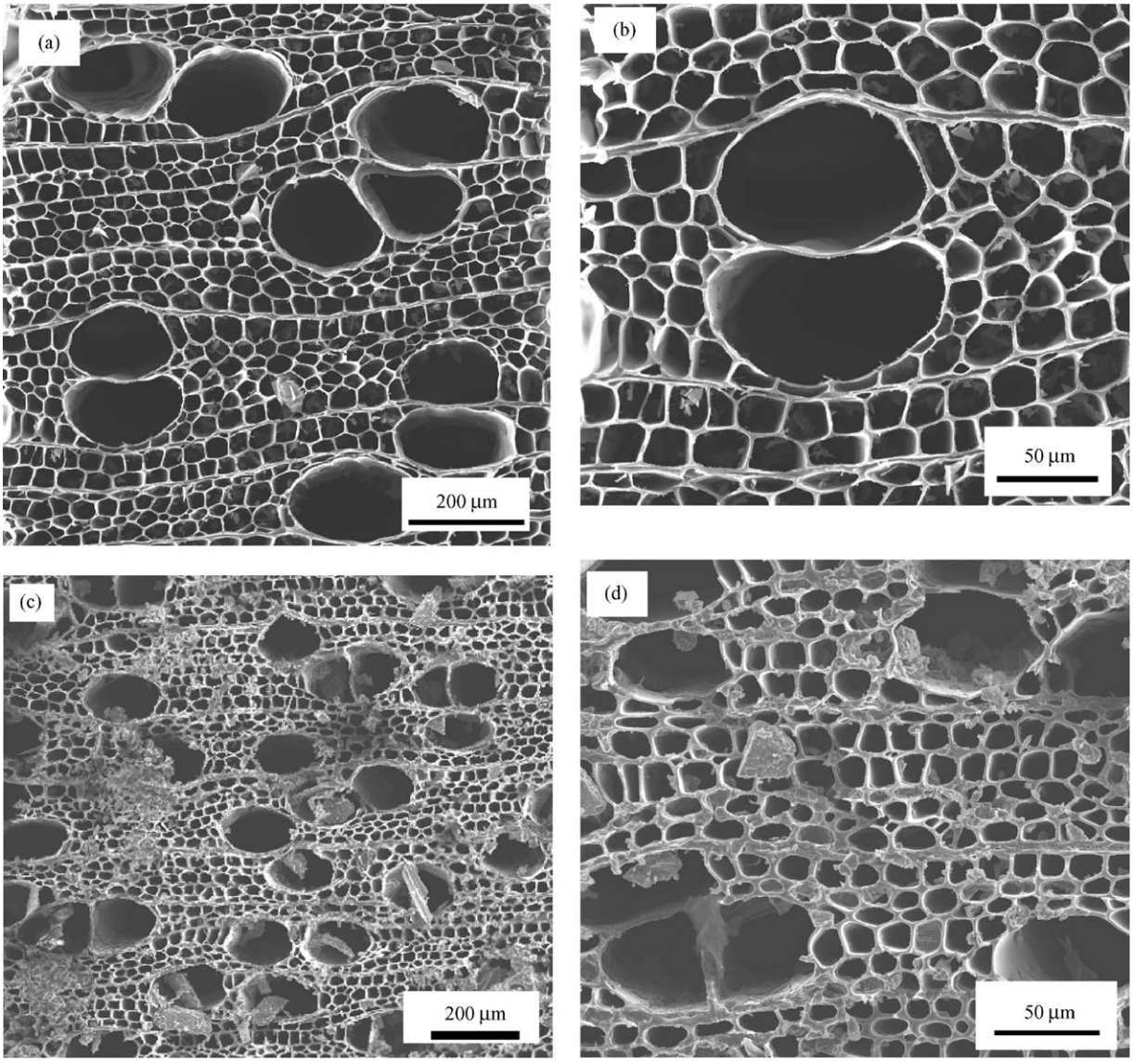

Fig. 4. Cross section microstructure of poplar after pyrolysis at 1000 °C×1 h (a,b) and after infiltration with Si at 1500 °C×2 h, sample 7 of Table 3 (c,d).

The amount of residual silicon in poplar and assembled poplar after infiltration (28.1 and 26.5 vol.% respectively) is higher than in obece (0–14 vol.%) and the final porosity is consequently lower (Table 1). Presence of residual silicon which closed small pores is confirmed by the SEM-EDS elemental analysis of the samples cross section. In assembled poplar silicon entered by capillarity also into the fractures between the wood layers formed during the pyrolysis. In addition a consistent thickening of the wall cells is also observed (Figs. 4c and d and 5b).

3.6. Compressive tests of infiltrated samples

The compressive strength of infiltrated samples is revealed in Table 4. The average compressive strength in the axial direction (i.e. with the channels oriented in the same direction of the load) is 55 MPa for obece and 108 for poplar. Assembled poplar differs slightly to poplar. In all the tested samples the compressive strength in the opposite direction (i.e. with the channels perpendicularly oriented to the load) is 8–10 times smaller.

Comparing the strength data in respect with porosity, we find that the strength decreases with increasing porosity. To give an idea about a possible underlying trend, the data are shown in (Fig. 6) with an interpolating exponential curve, which is normally used to describe the strength–porosity relationship.[17]

The lower strength in the axial direction exhibited by infiltrated obece compared to poplar and assembled poplar is related to the higher amount of final porosity in obece. Poplar and assembled poplar have a higher

Table 4
Compressive strength of infiltrated samples (1500 °C/120 min)

Sample	Compr. strength[a] (MPa)	Compr. strength[b] (Mpa)
Obece (30 MPa)	55.9±24.4	7.0±2.8
Poplar (31MPa)	108.0±21.7	8.2±3.9
Assembled poplar	105.0±19.7	9.0±2.5

[a] Channels parallel to the compression direction.
[b] Channels perpendicular to the compression direction.

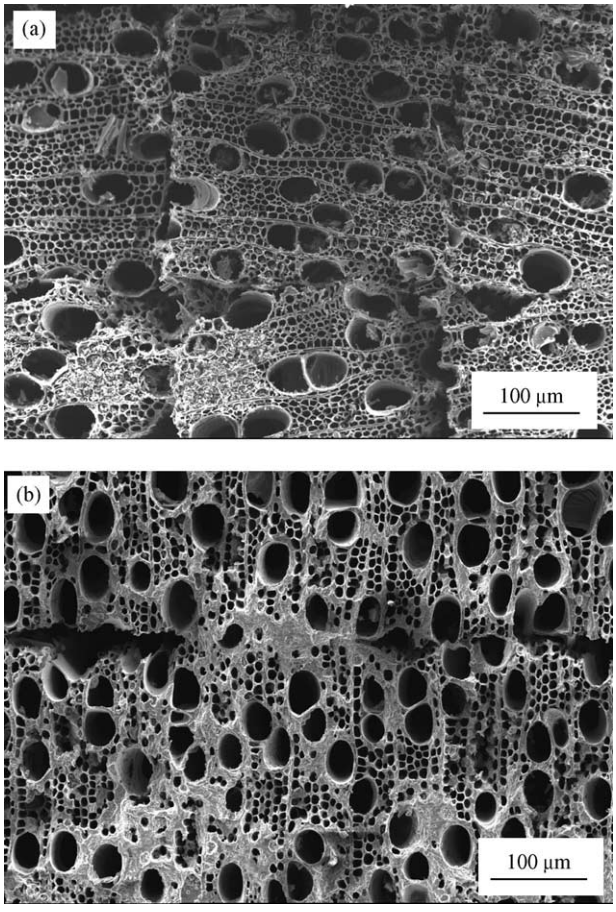

Fig. 5. Cross section microstructure of assembled poplar after pyrolysis at 1000 °C×1 h (a) and after infiltration with Si at 1500 °C×2 h, sample 8 of Table 3 (b).

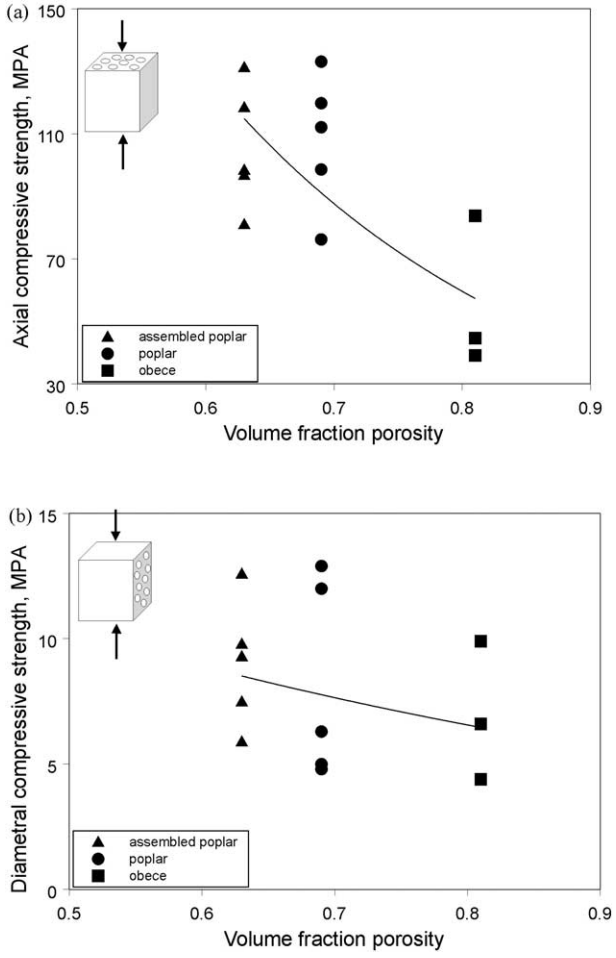

Fig. 6. Strength data interpolated with an exponential curve normally used to describe strength–porosity curve. Strength measured in the axial (a) and the longitudinal (b) directions.

compressive strength despite the fact that they contain a higher amount of residual silicon compared to obece. Finally the strength value of assembled poplar is similar to that of poplar despite the numerous fractures which were observed along the interfaces between the wood layers after the pyrolysis. During the infiltration process most of these fractures were closed by the silicon entering by capillarity, thus increasing the strength of the final material.

4. Conclusions

Porous SiC is obtained through a ceramization process based on the infiltration with liquid silicon of carbon templates formed by pyrolysed wood. Three types of woods are tested, obece, poplar and assembled poplar. The best processing parameters for infiltration are 1500 °C×2 h under flowing argon and with a slight excess of silicon, about 20 wt.% more than the stoichiometric quantity needed for the complete conversion of the carbon template to SiC. Under these conditions porous β-SiC with a crack-free microstructure which mimics the microstructure of the original wood and with a low amount of residual silicon, is obtained.

With obece as the starting material porous SiC with no residual silicon is obtained, whereas with poplar and assembled poplar the residual silicon in the infiltrated template is 28.1 and 26.5 vol.%, respectively. Residual silicon fills the smaller pores and decreases the total porosity.

Compressive strength values are related to the final porosity of the SiC material.

Acknowledgements

The authors wish to thank Cesare Melandri for the mechanical tests and Stefano Guicciardi for the helpful discussion on compressive strength data.

References

1. Greil, P., Biomorphous ceramics from lignocellulosics. *J. Eur. Ceram. Soc*., 2001, **21**, 105–118.
2. Ota, T., Takahashi, M., Hibi, T., Ozawa, M., Suzuki, S. and Hikichi, Y., Biomimetic process for producing SiC "wood". *J. Am. Ceram. Soc*., 1995, **78**, 3409–3411.
3. Greil, P., Lifka, T. and Kaindl, A., Biomorphic cellular silicon carbide ceramics from wood: I. Processing and microstructure. *J. Eur. Ceram. Soc*., 1998, **18**, 1961–1974.
4. Greil, P., Lifka, T. and Kaindl, A., Biomorphic celllular silicon carbide ceramics from wood: II. Mechanical properties. *J. Eur. Ceram. Soc*., 1998, **18**, 1975–1983.
5. Byrne, C. E. and Nagle, D. C., Carbonized wood monoliths—characterization. *Carbon*, 1997, **45**, 267–273.
6. Byrne, C. E. and Nagle, D. C., Carbonization of wood for advanced materials applications. *Carbon*, 1997, **45**, 259–266.
7. Vogli, E., Mukerji, J., Hoffman, C., Kladny, R., Sieber, H. and Greil, P., Conversion of oak to cellular silicon carbide ceramic by gas-phase reaction with silicon monoxide. *J. Am. Ceram. Soc*., 2001, **84**, 1236–1240.
8. Vogt, U., Herzog, A. and Klingner, R., Porous SiC Ceramics with Oriented Structure from Natural Materials. In *Proceedings of the 26th Annual International Conference on Advanced Ceramics & Composites*, The American Ceramic Society, 13–18 January 2002, Cocoa Beach, FL (in press).
9. Martínez-Fernández, J., Valera-Feria, F. M. and Singh, M., High temperature compressive mechanical behavior of biomorphic silicon carbide ceramics. *Scripta Mater*., 2000, **43**, 813–818.
10. Hillig, W. B., Melt infiltration approach to ceramic matrix composites. *J. Am. Ceram. Soc*., 1988, **71**, C96–C99.
11. Shin, D.-W., Park, S. S., Choa, Y.-H. and Niihara, K., Silicon/siliconcarbide composites fabricated by infiltration of a silicon melt into charcoal. *J. Am. Ceram. Soc*., 1999, **81**, 3251–3253.
12. Sieber, H., Vogli, E. and Greil, P., Biomorphic SiC-ceramic manifactured by gas phase infiltration of pine wood. In *Ceramic Engineering and Science Proceedings*, Vol. 22, Issue 4, The Am. Ceram. Society, ed. M. Singh, T. Jessen, 2001, pp. 109–115.
13. Tanaka, H. and Iyi, N., *J. Ceram. Soc. Jpn*, 1991, **101**, 1281.
14. ICCD Card no. 27-1402.
15. Giordano, G., *Tecnica delle costruzioni in legno*. Hoepli, Italy, 1999.
16. Heuer, A. H. and Lou, V. L. K., Volatility diagrams for silica, silicon nitride, and silicon carbide and their application to high-temperature decomposition and oxidation. *J. Am. Ceram. Soc*., 1990, **73**, 2785–3128.
17. Rice, R. W., Evaluation and extension of physical property-porosity models based on minimum solid area. *J. Mat. Sci*., 1996, **31**, 102–118.